J. Phys. B: At. Mol. Phys. 15 (1982) 1433–1441. Printed in Great Britain

Two-parameter coincidence measurements of bremsstrahlung, electron–electron bremsstrahlung, and K-shell ionisation for 300 keV electron impact

M Komma and W Nakel

Physikalisches Institut, Universität Tübingen, D-7400 Tübingen, West Germany

Received 30 October 1981, in final form 19 January 1982

Abstract. An electron beam of 300 keV was directed on to thin target foils (C, Cu, Ag, and Au) to investigate the processes of electron–nucleus bremsstrahlung, electron–electron bremsstrahlung, and K-shell ionisation. Using a two-parameter arrangement the outgoing electrons from all these processes were detected in coincidence with the emitted bremsstrahlung and K x-ray photons, respectively, as a function of electron and photon energies for fixed detector angles. So it was possible to measure the triply differential cross sections of the processes of electron–nucleus bremsstrahlung and electron–electron bremsstrahlung and the doubly differential cross section of K-shell ionisation simultaneously. A comparison with theoretical calculations is given.

1. Introduction

An electron beam passing through matter produces electron–nucleus bremsstrahlung, electron–electron bremsstrahlung and characteristic x-rays via inner-shell ionisation. The bremsstrahlung processes have continuous spectra both in photon energy (E_γ) and outgoing electron energy (E_e), the ionisation is accompanied by a characteristic line spectrum and a continuous electron spectrum (Auger electrons are not considered in this work).

Using a two-parameter arrangement the outgoing electrons of these processes were detected in coincidence with the emitted photons as a function of outgoing electron and photon energies for fixed detector angles. In this way it was possible to measure simultaneously the triply differential cross sections ($d^3\sigma/d\Omega_e d\Omega_\gamma dE_e$) of the processes of electron–nucleus (e–n) bremsstrahlung and electron–electron (e–e) bremsstrahlung and the doubly differential cross section ($d^2\sigma/d\Omega_e dE_e$) of K-shell ionisation as a function of the outgoing electron energy. Thus much information about inelastic collision processes of relativistic electrons results from the two-parameter coincidence measurement. The expected kinematical curves of the processes are delineated in figure 1. Here, the curve of the e–e bremsstrahlung is calculated for a collision of an incident electron with a free electron initially at rest (approximately true for low-Z atoms). With the conservation laws one obtains for the energy of the emitted photon

$$E_\gamma = \frac{\varepsilon_0 - \varepsilon + 1 - \varepsilon_0\varepsilon + \boldsymbol{p}_0\boldsymbol{p}}{\varepsilon_0 - \varepsilon + 1 - (\boldsymbol{p}_0 - \boldsymbol{p})\hat{\boldsymbol{k}}} mc^2$$

0022-3700/82/091433+09$02.00

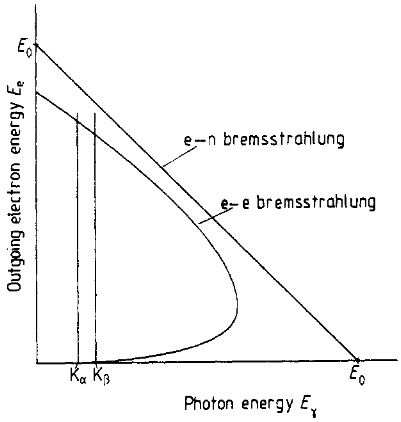

Figure 1. Kinematics of the measured processes. According to energy conservation the e–n bremsstrahlung is situated along the straight line $E_e = E_0 - E_\gamma$ where E_0 is the primary electron energy. The curve for the e–e bremsstrahlung has an angle dependent shape and the quantum energy lies below that of e–n bremsstrahlung because the second electron carries away energy. In the coincidence experiment the events of the K-shell ionisation appear at the energies of the K_α and K_β lines.

where ε_0 and ε are the total energies of the incident and detected electron, respectively, in units of the rest energy mc^2, and $\boldsymbol{p}_0$ and $\boldsymbol{p}$ are the corresponding momenta in units of mc. $\hat{\boldsymbol{k}}$ is the unit vector in the direction of the emitted photon.

For the triply differential cross section of e–n bremsstrahlung only approximate calculations have been available until now. The classical Bethe–Heitler formula (1934) describes the production of bremsstrahlung in the first Born approximation. The region of validity is roughly $\alpha Z/\beta \ll 1$, where $\alpha = 1/137$ is the fine-structure constant, β the velocity of the outgoing electron in units of the velocity of light, and Z is the atomic number of the target atom. The region of validity of the calculations of Elwert and Haug (1969) using Sommerfeld–Maue wavefunctions can be expressed by $\alpha Z \ll 1$. This does not depend on the energy of the incident electron or of the photon energy. Since the region of validity of the calculations is not sharply limited by the above inequalities, experimental tests are important. Numerical calculations of the triply differential cross sections with partial waves after Tseng and Pratt (1971) are not available so far.

A short summary of previous measurements of the triply differential cross section is given by Nakel (1980).

Only very few experimental results are available on e–e bremsstrahlung generated by collisions with an orbital electron of the atom. The e–e bremsstrahlung in general gives such a small contribution to the total bremsstrahlung emission that it is not taken into account in most bremsstrahlung measurements. Especially in the case of high-Z targets, the experiments give almost pure nuclear bremsstrahlung, since the electron–nucleus bremsstrahlung is closely proportional to Z^2, whereas the e–e bremsstrahlung is proportional to the number of electrons.

Several experimental investigations (cf Rester (1968)) show that it is difficult to isolate the e–e bremsstrahlung component from the total spectrum by observing only the photon spectrum. Therefore Nakel and Pankau (1973) used the electron–photon coincidence technique to differentiate exactly between the two bremsstrahlung components by means of a kinematically overdetermined measurement and measured the triply differential cross section and the angular correlation (Nakel and Pankau 1975) using a target with low-Z atoms (carbon).

In this work we have measured the spectral distribution of the e–e bremsstrahlung process for fixed angles of outgoing electrons and photons, and targets of different atomic number. We compare our measurements with a calculation of Haug (1975).

For the investigation of inner-shell ionisation processes the measurement of multiply differential cross sections will provide a more stringent way to distinguish between various theoretical approximations. However, because of the difficulties of the measurements there are still very few experiments on multiply differential cross sections for inner-shell ionisation by electron impact. For relativistic electron energies only Quarles and Faulk (1973) and Komma and Nakel (1979) have published experimental data on doubly differential cross sections for K-shell ionisation.

We compare our measurements with calculations of Das (1972), Das and Konar (1974), and Moisewitsch and Norrington (1979).

2. Experimental procedure

A schematic diagram of the experimental arrangement is shown in figure 2. The electron beam from a 300 kV accelerator was focused to a 1 mm diameter spot on target placed at the centre of a vacuum chamber (50 cm diameter). The targets consisted of evaporated films of carbon, copper, silver (self-supporting) and gold (on formvar backing) with thicknesses between 40 and 60 μg cm^{-2}.

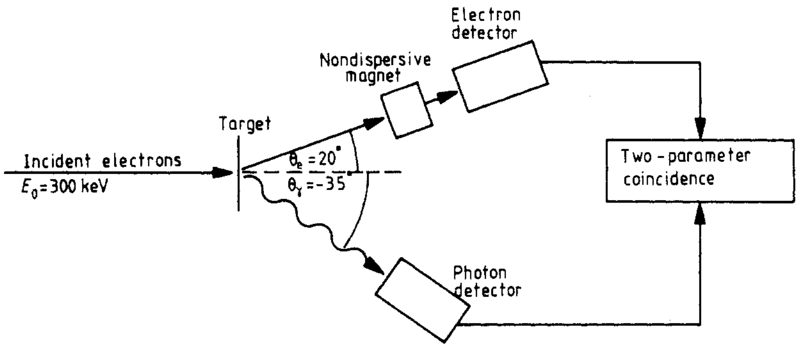

Figure 2. Schematic diagram of the experimental arrangement.

The bremsstrahlung photons and characteristic x-rays from the target leave the chamber through a plastic window (50 μm) before entering a high purity germanium detector (Schlumberger EG pp 800 H) set up at −35° with respect to the incident electron beam. Electrons scattered in this direction were deflected by permanent magnets to avoid bremsstrahlung production in the window.

The outgoing electrons were observed with a surface barrier detector (Ortec TE-013-50-500) at a scattering angle of 20°. It was essential to avoid detecting elastically scattered electrons since the count rate for these is orders of magnitude higher than that of the inelastic processes. In order to eliminate the elastically scattered electrons before reaching the detector but to transmit the inelastically scattered electrons within a broad energy range a triply focusing (non-dispersive) magnet (Komma 1978) was inserted between the defining aperture and the surface barrier detector. With this system 100% of the outgoing electrons were transmitted within an energy band of 40 to 200 keV and a solid angle of 1.36 msr. The energy resolution of the cooled detector was 5 keV.

The timing pulses of both detectors were fed into a time-to-pulse height converter (Ortec Model 467) via constant-fraction discriminators (Canberra Model 1326B) and a window of a single-channel analyser was set on this coincidence peak. The amplified energy signals of both detectors were gated by the fast coincidences and fed to the two analogue–digital converters of a two-parameter multichannel analyser (Wenzel MAC 4000). The two-parameter spectra were stored in the core memory as a 64 × 64 channel matrix. With the stand-alone-system SAM, installed by Grammer (1978) in a PDP 11/05 computer, the matrices were transferred in cycles of about 1 h from the multichannel analyser to the PDP 11/05 and were stored in cycles of about 10 h on the disc of a PDP 11/45 for further data processing.

To determine the two-parameter spectrum of random coincidences with a small statistical error, we have measured the single (one-parameter) electron and photon spectra separately between the two-parameter runs and calculated the corresponding matrix by multiplication. The matrix—obtained with a high counting rate—was normalised with the measured total number of random coincidences from the timing spectrum.

The beam current was measured with a Faraday cup and found to be 10^{-8} A. The target thickness was determined from measurements of the energy loss of α particles passing through the foil. The conversion factor was taken from the tables of Barkas and Berger (1964). Moreover, the product of target thickness and beam current was checked by measuring the elastically scattered electrons with a surface barrier detector.

The photon detector efficiency was measured using calibrated radioactive sources (Ba^{133}, Ta^{182}) and interpolated for the energies of interest. The spectra were deconvoluted with an electron detector efficiency of 0.85 (cf Berger et al 1969).

3. Results and discussion

In figures 3(*a*) and (*b*) and 4(*a*) and (*b*) plots of two-parameter spectra of true coincidences are shown measured for targets of carbon, copper, silver, and gold (cf figure 1 for the kinematics). The diagonal feature in all plots is due to e–n bremsstrahlung. For carbon (figure 3(*a*)), the e–e bremsstrahlung is well separated from the e–n bremsstrahlung. Its kinematical curve in the E_γ–E_e plane which depends on the angles of observation corresponds to a collision between free electrons. With increasing atomic number of the target the ratio of e–e bremsstrahlung to e–n bremsstrahlung decreases and then the e–e bremsstrahlung disappears in the low-energy tail and the Compton continuum produced by the dominant e–n bremsstrahlung. Moreover, the stronger binding of the electrons causes a smear out of the kinematics for free particles.

For silver and gold (figures 4(*a*), (*b*)), the energy of the characteristic K x-rays is high enough to be detected with sufficient good time resolution, which results in the observation of the corresponding lines.

For comparison with theory we have projected the number of true coincidences of the processes on the E_e axis and determined the relevant cross sections from the number of coincidences, the beam current, the target thickness, the solid angles, and the efficiencies of the detectors. The results for the bremsstrahlung processes are shown in figures 3(*c*) and (*d*) and 4(*c*) and (*d*). The error bars represent the mean square root of the statistical error and the estimated systematic errors. The systematic errors amount to about 20%, the main contribution coming from the uncertainty in the response of the Ge detector (10%) and the target thickness (5–8%).

Multiple scattering has not been taken into account, since for the chosen parameters the theoretical cross sections vary only slowly with the detection angles, so that the resulting error should be small even for high Z.

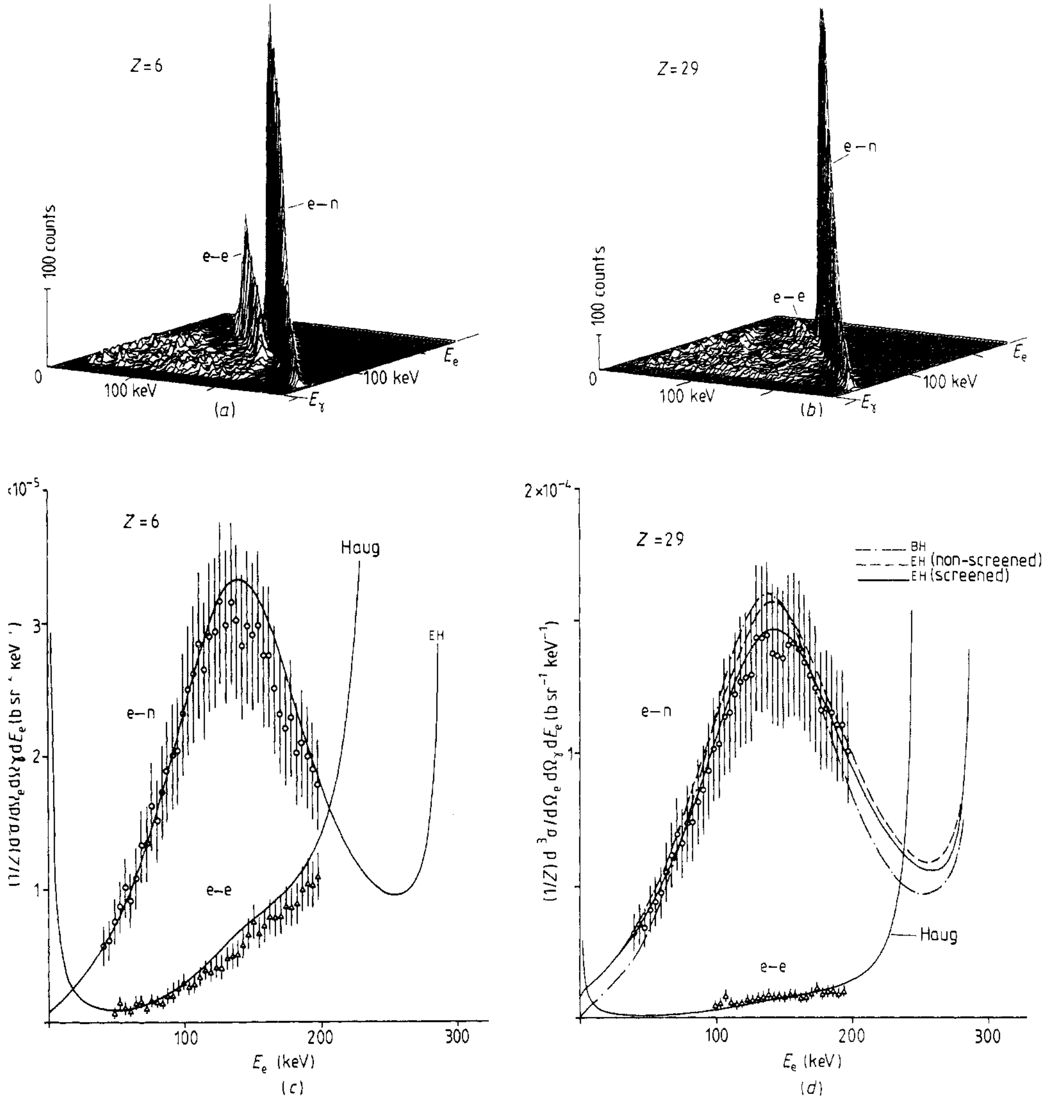

Figure 3. Electron–photon coincidence spectra for (*a*) carbon, (*b*) copper, and the pertinent triply differential cross sections (*c*), (*d*) of e–n bremsstrahlung and e–e bremsstrahlung. In the coincidence spectra the random coincidences are subtracted. The remaining events at low energies are due to electron backscattering and Compton scattering in the detectors. The theoretical curves are calculated after formulas of Bethe–Heitler (BH), Elwert–Haug (EH) and Haug.

3.1. *e–n bremsstrahlung*

The measured triply differential cross sections for the e–n bremsstrahlung are compared with two approximate calculations: the Bethe–Heitler (BH) formula (1934) and the Elwert–Haug (EH) calculation (1969).

For small Z, the BH ($\alpha Z \ll \beta$) and the EH ($\alpha Z \ll 1$) calculations give practically the same results. Therefore, for carbon, only the EH calculation is shown in figure 3(*c*).

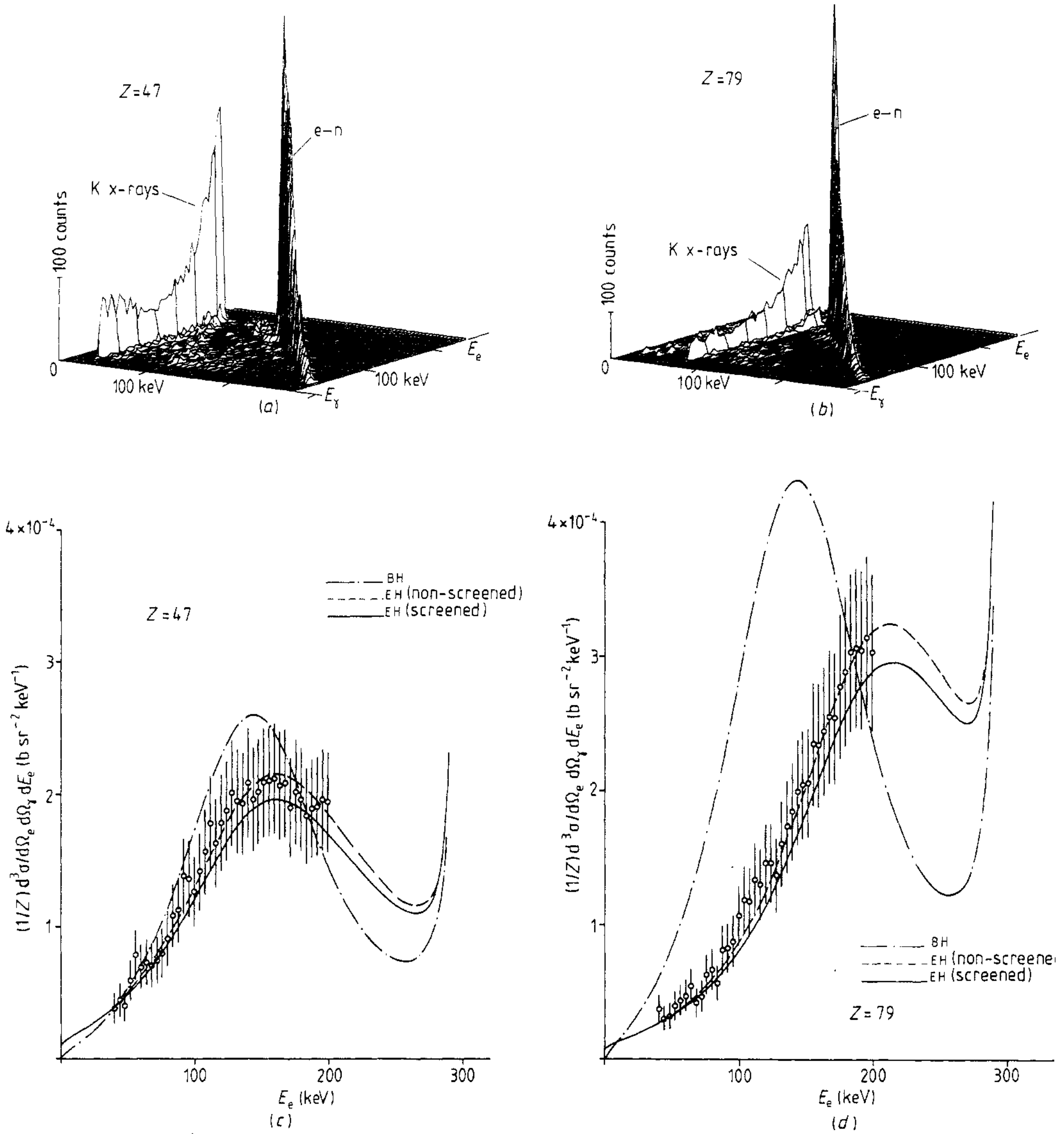

Figure 4. Electron–photon coincidence spectra for (*a*) silver, (*b*) gold, and the pertinent triply differential cross sections (*c*), (*d*) of e–n bremsstrahlung. In the coincidence spectra the random coincidences are subtracted. The theoretical curves are calculated after formulas of Bethe-Heitler (BH) and Elwert–Haug (EH).

The measured cross section, especially the position of the maximum, is in good agreement with the theory. For copper, the two calculations differ noticeably but still lie within the experimental errors (figure 3(*d*)). However, with increasing Z the BH calculations deviate more and more from the measured curves. In this calculation the position of the maximum is independent of Z, whereas in the EH calculation the maximum is shifted towards higher electron energies with increasing atomic number in accordance with the measured curves. The good agreement of the EH calculation with the measurements even at high Z shows, that the theory using Sommerfeld–Maue wavefunctions is a good approximation at the present parameters.

In previous measurements of the triply differential cross section for gold with other scattering parameters appreciable deviations from the EH calculation were found (Kreuzer and Nakel 1971, Faulk and Quarles 1974, Aehlig et al 1977). Therefore it is desirable to extend the measurements to determine the region of validity of the calculations. It is hoped that numerical calculations with partial waves (Tseng and Pratt 1971) will be available in the near future.

3.2. e–e bremsstrahlung

We compare our measurements of the triply differential cross section of e–e bremsstrahlung on carbon and copper with a calculation of Haug (1975) for collisions between free electrons (figures 3(*c*), (*d*)). The calculation of the cross section in Born approximation is achieved by a straightforward application of quantum electrodynamics. However, compared with the Bethe–Heitler formula of the corresponding process in the Coulomb field of a nucleus, these expressions are extremely complicated owing to recoil and exchange effects. Mack and Mitter (1973) who solved the problem by using computer programs for formula manipulations and Haug (1975) who used the traces calculated by Anders (1964) obtained identical results. The agreement of the experimental cross section with the calculation for free electrons is quite good.

We have not evaluated the measurements on the silver and gold targets because the number of e–e bremsstrahlung events on the kinematical curve was too low. Here, due to the strong binding and broad momentum distribution of the inner-shell electrons (momentum p_2) a smear out of the free electron kinematic will appear. For a rough estimation of the form of the smear out the momentum distribution $|\psi_H(p_2)|^2$ has been integrated over the direction of the non-detected electron using the hydrogen-like wavefunction given by Fock (1936) and the kinematics for the free e–e bremsstrahlung (Komma 1980). The result of the calculation of the integral for all electrons of the K, L, and M shell of gold is shown in figure 5. A certain check of the reliability of this estimation is, that the following limit cases are reproduced in a reasonable form: the form of the spectral distribution of the outgoing electrons for pure ionisation ($E_\gamma = 0$), to be seen above the E_e axis of figure 5, corresponds to the curve of the

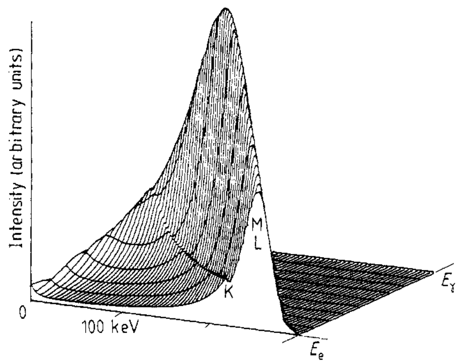

Figure 5. Calculated smear out of the e–e bremsstrahlung of gold for all electrons of the K, L, and M shells. $Z = 79$, $E_0 = 300$ keV, $\theta_e = 20°$, $\theta_\gamma = -35°$.

ionisation cross section in figure 6. For the outer electrons with low binding energy the kinematical curve of the free e–e bremsstrahlung given in figure 1 is reproduced in a broadened form in figure 5. For K electrons with high binding energy the maximum of the e–e bremsstrahlung lies above a straight line in the E_e–E_γ plane.

A correct treatment of the bremsstrahlung process on bound electrons is extremely difficult and has not been available until now.

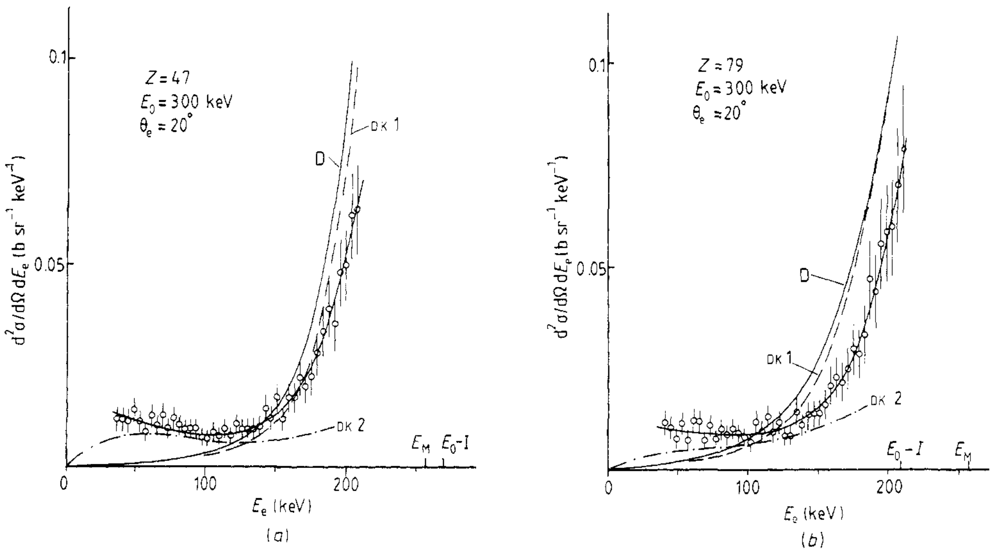

Figure 6. Doubly differential cross section for K-shell ionisation of: (*a*) silver, (*b*) gold, against the kinetic energy E_e of the outgoing electrons. E_0, kinetic energy of the incident electrons; θ_e, scattering angle; E_M, Møller energy; *I*, binding energy. The theoretical curve labelled D is a calculation after a formula of Das (1972). For the calculation of curves labelled DK the triply differential cross section of Das and Konar (1974) was integrated over the direction of the ejected electron (DK 1) and over the direction of the scattered electron (DK 2) as proposed by Konar (1975).

3.3. K-shell ionisation

Figure 6 shows the doubly differential cross sections of K-shell ionisation as a function of outgoing electron energy which was discussed by Komma and Nakel (1979). In the meantime we have computed the corresponding cross sections after the formula of Moiseiwitsch and Norrington (1979) and found that the results coincide with the calculation of Das (1972), that is with the curve labelled D. The overestimation of the cross section by the theoretical values is the more surprising, as the experimental points include the events of e–e bremsstrahlung integrated over the energy and angle of the photons not detected.

Further measurements of the ionisation process are in progress.

We would like to thank Professor H Krüger for his support of this work. We are very grateful to Professor E Haug for valuable discussions and to Dr J N Das for helpful correspondence.

References

Aehlig A, Metzger L and Scheer M 1977 *Z. Phys.* A **281** 205
Anders T 1964 *Nucl. Phys.* **59** 127
Barkas W H and Berger M J 1964 *Natl Acad. Sci.—Natl Res. Council Publ.* **1133** 103
Berger M J, Seltzer S M, Chappell S E, Humphreys J C and Motz J W 1969 *Nucl. Instrum. Methods* **69** 181
Bethe H and Heitler W 1934 *Proc. R. Soc.* A **146** 83
Das J N 1972 *Nuovo Cim.* B **12** 197
Das J N and Konar A N 1974 *J. Phys. B: At. Mol. Phys.* **7** 2417
Elwert G and Haug E 1969 *Phys. Rev.* **183** 90
Faulk J D and Quarles C A 1974 *Phys. Rev.* A **9** 732
Fock V 1936 *Z. Phys.* **98** 145
Grammer A 1978 *Diplomarbeit* Tübingen
Haug E 1975 private communication, cf *Z. Naturforsch.* **30**a 1099
Komma M 1978 *Nucl. Instrum. Methods* **154** 271
—— 1980 *Dissertation* Tübingen
Komma M and Nakel W 1979 *J. Phys. B: At. Mol. Phys.* **12** L587
Konar A N 1975 *Acta Phys. Acad. Sci. Hung.* **38** 337
Kreuzer K and Nakel W 1971 *Phys. Lett.* **34A** 407
Mack D and Mitter H 1973 *Phys. Lett.* **44A** 71
Moiseiwitsch B L and Norrington P H 1979 *J. Phys. B: At. Mol. Phys.* **12** L283
Nakel W 1980 *Coherence and Correlations in Atomic Collisions* ed H Kleinpoppen and J F Williams (New York: Plenum)
Nakel W and Pankau E 1973 *Phys. Lett.* **44A** 65
—— 1975 *Z. Phys.* A **274** 319
Quarles C A and Faulk J D 1973 *Phys. Rev. Lett.* **31** 859
Rester D H 1968 *Nucl. Phys.* A **118** 129
Tseng H K and Pratt R H 1971 *Phys. Rev.* A **3** 100